Fuel 253 (2019) 772–780

Contents lists available at ScienceDirect

Fuel

journal homepage: www.elsevier.com/locate/fuel

Hydrogen concentration effects on swirl-stabilized oxy-colorless distributed combustion

Serhat Karyeyen[a,b], Joseph S. Feser[a], Ashwani K. Gupta[a,*]

[a] Mechanical Engineering Department, University of Maryland, College Park, MD 20742, USA
[b] Department of Energy Systems Engineering, Faculty of Technology, Gazi University, Teknikokullar, 06500 Ankara, Turkey

ARTICLE INFO

Keywords:
Colorless distributed combustion
Oxy-fuel combustion
Low CO emission
Gas turbine combustion

ABSTRACT

Oxy-colorless distributed combustion is a novel combustion technique to achieve more uniform and controlled thermal field, enhance flame stability, and reduce emissions including combustion noise. Colorless distributed combustion (CDC) conditions was achieved through controlled entrainment of hot reactive gaseous species. This allowed for reduction of oxygen concentration to provide improved mixture preparation for distributed combustion with the reaction zone distributed across the entire volume of the combustor. In this study, oxy-colorless distributed combustion was examined for fuel flexibility using different mixtures of methane and hydrogen diluted with 10% each of N_2 and CO_2 to represent low heating value fuels. The oxidizer used was an O_2-CO_2 mixture that eliminated the formation of NOx from the combustor. The evolved OH* chemiluminescence signatures were recorded for various hydrogen concentrations in the fuel at equivalence ratios in the range of 0.6–0.9 under distributed combustion condition. At $\Phi = 0.9$, transition to CDC initiated at oxygen concentrations of 17%, 19% and 21% for fuels having a hydrogen concentration of 60%, 50% and 40% (on volume basis), respectively. Differences in transition point were attributed to higher flame speed associated with more hydrogen in the fuel. Gaseous fuel having high hydrogen concentration provided more distributed OH* flame structures at lower oxygen concentration while the flame stability enhanced at higher oxygen concentration. Oxy-colorless conditions provided only 10–30 ppm CO even at high oxygen concentration and high (0.9) equivalence ratio. The results showed fuel flexibility from different heating value gaseous fuels having high hydrogen content. The results provided very low CO emission and enhanced flame stability under oxy-colorless distributed combustion for the low heating value fuels using O_2-CO_2 mixture as the oxidant.

1. Introduction

Continuous increase in consumption of fossil fuels has caused growing concerns on environment and climate issues. This challenge dictates combustion scientists/engineers to seek novel combustion methods to utilize fossil fuels at high combustion efficiency, and mitigate pollutants emission, including greenhouse gas emissions which contribute to environmental harm and global warming. Oxy-fuel combustion offers an alternative method to convert chemical energy in fossil fuels to heat and electricity. During this process, carbon dioxide and water vapor are produced as the primary combustion products. The production of higher levels of CO_2 can be managed via carbon capture and sequestration (CCS) technologies. Water is condensed out leaving carbon dioxide, which can be captured, compressed to provide a supercritical fluid, then transported and stored [1]. Alternative methods for the capture of carbon dioxide include, air-fired combustion with post-combustion CO_2 capture or gasification/combined cycle power plants with pre-combustion CO_2 capture. Specific CCS technology applicable will depend on the prevalent technical and economic conditions [1]. Suitability of oxy-fuel combustion with CO_2 capture offers a good opportunity for fossil fuel combustion with simultaneous pollutants reduction and higher efficiency. In oxy-fuel combustion technique an O_2-CO_2 mixture is used as an oxidizer instead of air. In this way, the nitrogen present in the product stream is eliminated, mitigating NO_x emission due to the absence of nitrogen in air.

Characteristics of oxy-fuel combustion are different compared to conventional combustion in terms of flame temperature, flame speed, and other flame characteristics. Flame temperature, for example, is generally higher due to absence of free nitrogen which absorbs much of the heat generated. Adiabatic flame temperature for oxy-fuel combustion is higher than that of normal combustion which uses air as the oxidizer. Higher flame temperature necessitates introduction of

* Corresponding author.
E-mail address: akgupta@umd.edu (A.K. Gupta).

https://doi.org/10.1016/j.fuel.2019.05.008
Received 3 March 2019; Received in revised form 1 May 2019; Accepted 2 May 2019
Available online 20 May 2019
0016-2361/

combustion products into the reactant stream to reduce peak flame temperature and lower flame speed to support a stable flame under oxy-fuel combustion [2]. Higher temperatures pose challenges from increased flame speed in oxy-fuel combustion as compared to conventional flames [3]. This requires one to use either higher inlet velocities in the mixture, introduction of a non-reactive gas in order to handle the excess heat, or some combination of the two to stabilize the flame. Therefore, the reintroduction of combustion products, mostly CO_2 and steam in oxy-fuel combustion, enables an increase in mixture velocity and heat capacity to mitigate flame fluctuations and instabilities present at high temperatures and flame speeds [4].

Many studies are reported in the literature on oxy-fuel combustion. Galmiche et al. [4] investigated dilution effects of methane on laminar flame speed under premixed conditions. They used several diluents and concluded that adding diluents lowers flame speed. Nemitallah and Habib [5] investigated oxy-fuel combustion of methane in a model gas turbine combustor. They concluded that the flame stability was greatly affected when the oxygen concentration in the oxidizer was reduced below 25% and the flame extinguished below 21% oxygen concentration under all conditions. Heil et al. [6] examined the chemical effect of CO_2-methane combustion under oxy-flame conditions. The results showed higher levels of CO for O_2-CO_2 mixture than that for O_2-N_2 case. Ilbas et al. [7] used low calorific value syngases as fuel using pure oxygen and compared the results with conventional combustion, using normal air. They reported higher flame temperatures for all conditions compared to the conventional air case. Williams et al. [8] conducted an experimental study on the burning of fuels (pure methane, H_2-rich and H_2-lean syngas mixtures) using air and O_2-CO_2 mixtures as oxidizers. They concluded that the presence of hydrogen in the syngas fuel mixtures yielded higher temperature flames [8]. Oxy-coal and biomass combustion studies are also available [9–15]. In these studies, coal [9], biomass/lignite blends [10], different types of pulverized biomass [11,12], co-firing of biomass and coal [13,15] and coal and biomass [14] were examined under different oxy-flame conditions. These studies concluded that oxy-fuel combustion highly affects the flame characteristics, flame temperature and pollutants emission.

To mitigate pollutants emission and improve combustion efficiency, some novel combustion techniques such as High Temperature Air Combustion (called HiTAC), FLOX (Flameless Oxidation), MILD (Moderate or Intense Low Dilution) combustion, and Colorless Distributed Combustion (CDC) and Volume Distributed Combustion (VDC) have been reported. Results on the operating range for different fuels under MILD oxy-combustion conditions are reported [16]. Krishnamurthy et al. [17] used an oxy-fuel burner under conventional and flameless conditions. The results showed significant changes in temperature distributions between predictions and measurements. Khalil and Gupta [18] also conducted the experimental study under oxy-colorless distributed combustion conditions. They also investigated the effect of colorless distributed combustion on flame signature [18–24], emission [18–26], acoustic and heat release [27] and flow field [28–30].

The available studies examined under MILD, FLOX, CDC or VDC conditions primarily focus on combustion of methane or LPG fuels, although other fuels (liquid and solid) have also been reported. Challenges lie in the combustion of gaseous fuels having high hydrogen content under oxy-fuel combustion, as the flame characteristics of the hydrogen-blended gaseous fuels are much different, with greatly increased flame temperature and flame speed for hydrogen enriched fuel than methane. Therefore, utilization of the gaseous fuels containing high hydrogen concentration is quite difficult under oxy-fuel combustion so that gas turbine combustors and industrial burners must be modified in order to burn hydrogen-containing fuels efficiently and effectively with further consequences to the combustor, system and the environment. CDC offers enhanced combustion stability while providing significantly lower pollutants emission without any modification to the combustion system hardware. Through controlled entrainment of hot reactive species prior to ignition into the fresh mixture, the reaction rate can be controlled to foster enhanced flame stability and mitigation of flame flashback and combustion instability. The reaction zone in CDC broadens over the entire volume of the combustor. Therefore, hydrogen-blended gaseous fuels can be utilized for industrial gas turbine application even at near stoichiometric equivalence ratios due to mitigation of hot spot zones and reduced air cooling requirements for the combustor and turbine blades. This study examines several gaseous fuel blends having different amounts of hydrogen and methane using a swirl-stabilized burner under oxy-colorless distributed combustion conditions. Mixtures of oxygen and carbon dioxide were used here as the oxidizer. The effect of hydrogen amounts in the fuel was investigated for transition to CDC using OH* chemiluminescence diagnostics. The role of using various O_2-CO_2 mixtures as the oxidizer instead of air on CO emission was examined. The equivalence ratios examined ranged from 0.9 to 0.6 that unraveled the role of oxidizer dilution without reducing the oxygen concentration.

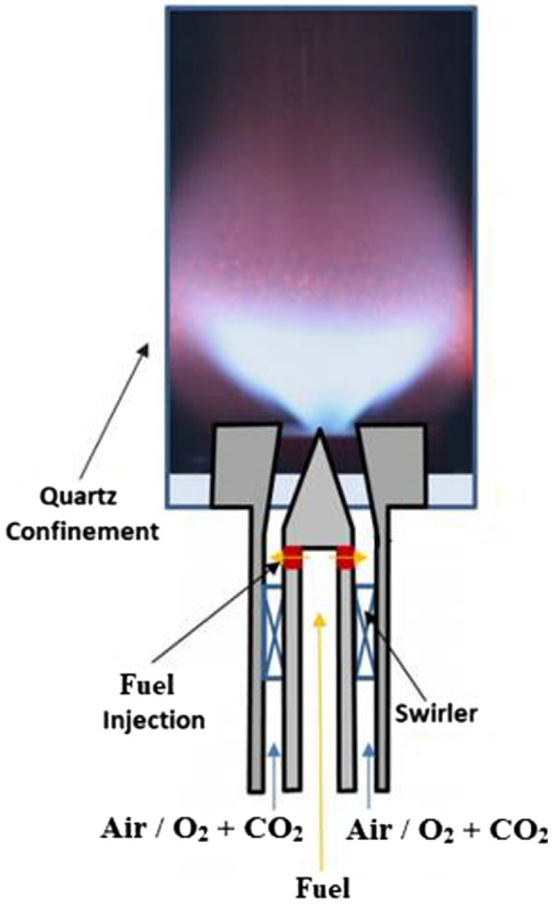

Fig. 1. A schematic diagram of the swirl-stabilized test combustor.

2. Experimental set-up

The combustor used is shown in Fig. 1; more details on the combustor used can be found elsewhere [31]. The set-up included fuel and oxidizer lines to feed gaseous fuels, air and/or O_2 + CO_2 mixtures to the burner. The combustor section constituted of a quartz tube having an internal diameter of 2.375 in. and a height of 7.874 in., which confined the burner.

Bottled gases of methane, hydrogen, nitrogen and carbon dioxide were used to prepare the desired fuel mixture. Compressed air, bottled oxygen and carbon dioxide were used to prepare the oxidizer mixtures necessary to achieve conventional or oxy-colorless distributed

Table 1
Gaseous fuels used (% volumetric basis) and their properties.

Fuel	N_2 [%]	CO_2 [%]	H_2 [%]	CH_4 [%]	Calorific Value [kJ/m^3]	Total Volumetric Flow Rate [L/min]
Gaseous Fuel 1	10	10	50	30	~16,140	12.0
Gaseous Fuel 2	10	10	60	20	~13,640	14.3
Gaseous Fuel 3	10	10	40	40	~18,640	10.5

Table 2
Experimental parameters.

Fuel Type	Equivalence Ratio	Air [L/min]	Oxidizer		Oxygen Concentration [%]
			O_2 [L/min]	CO_2 [L/min]	
Gaseous Fuel 1	0.9	53.95	N/A	N/A	21
		N/A	11.3	29.87–49.30	27.5–19
	0.8	60.69	N/A	N/A	21
		N/A	12.8	29.75–54.36	30–19
	0.7	69.36	N/A	N/A	21
		N/A	14.6	30.26–58.28	32.5–20
	0.6	80.92	N/A	N/A	21
		N/A	17.0	31.55–56.90	35–23
Gaseous Fuel 2	0.9	52.94	N/A	N/A	21
		N/A	11.1	33.36–54.29	25–17
	0.8	59.56	N/A	N/A	21
		N/A	12.5	32.95–61.03	27.5–17
	0.7	68.07	N/A	N/A	21
		N/A	14.3	37.70–65.14	27.5–18
	0.6	79.41	N/A	N/A	21
		N/A	16.7	44.00–66.72	27.5–20
Gaseous Fuel 3	0.9	55.53	N/A	N/A	21
		N/A	11.7	27.21–43.86	30–21
	0.8	62.48	N/A	N/A	21
		N/A	13.1	27.25–49.36	32.5–21
	0.7	71.40	N/A	N/A	21
		N/A	15.0	37.86–50.20	35–23
	0.6	83.30	N/A	N/A	21
		N/A	17.5	32.48–52.47	35–25

combustion condition. Each line included flowmeters to monitor the flowrates of fuel and oxidizer to the combustor. Laminar flow controllers used for monitoring air and nitrogen flow rates had accuracy of ± 0.8% of the reading and ± 0.2% of full scale reading that provided an overall accuracy of 1.5% of the reading. Methane, hydrogen, carbon dioxide and oxygen flowrates were also controlled by gravimetric flow controllers having an accuracy of 1.5% of full scale.

Conventional and oxy-colorless distributed flame structures were monitored using an ICCD (Intensified Charge-Couple Device) camera. The camera was also coupled to a narrow band filter (UV interference filter centered at 307 nm with a FWHM of ± 10 nm) that provided the OH* chemiluminescence signatures. A gas analyzer was used to determine concentrations of CO, CO_2 and O_2. Carbon monoxide, in ppm, was determined by non-dispersive infrared absorption method. Oxygen concentration was determined by galvanic method that allowed corrections for CO emission at (standard) 15% oxygen concentration. Repeatability of CO concentration measured was 0.5% of the full-scale reading.

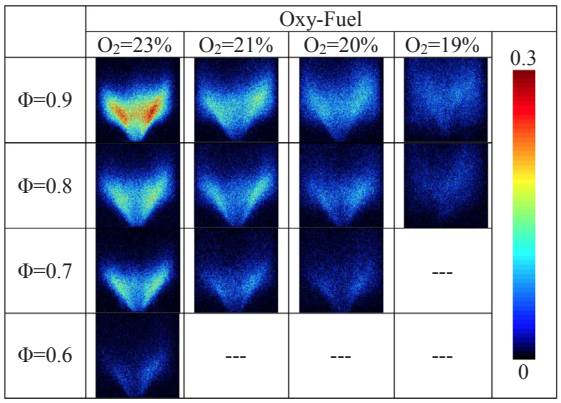

Fig. 3. OH* chemiluminescence signatures for gaseous fuel 1 at low intensity scale of 0–0.3.

3. Experimental conditions

The combustion behavior of several gaseous fuels having different concentrations of hydrogen and methane were examined in this study. Concentration of carbon dioxide and nitrogen in the gaseous fuel were kept the same for all the examined conditions. The hydrogen-enriched gaseous fuels used along with their properties are presented in Table 1.

Normal air was used to establish the baseline oxidizer case for the oxy-colorless distributed combustion. After which, the oxidizer was changed to an O_2-CO_2 mixture for the oxy-colorless distributed combustion condition. The oxygen concentration in the oxidizer was also changed until reaching the flammability limits for the gaseous fuels used. Table 2 presents experimental parameters for all the combustion

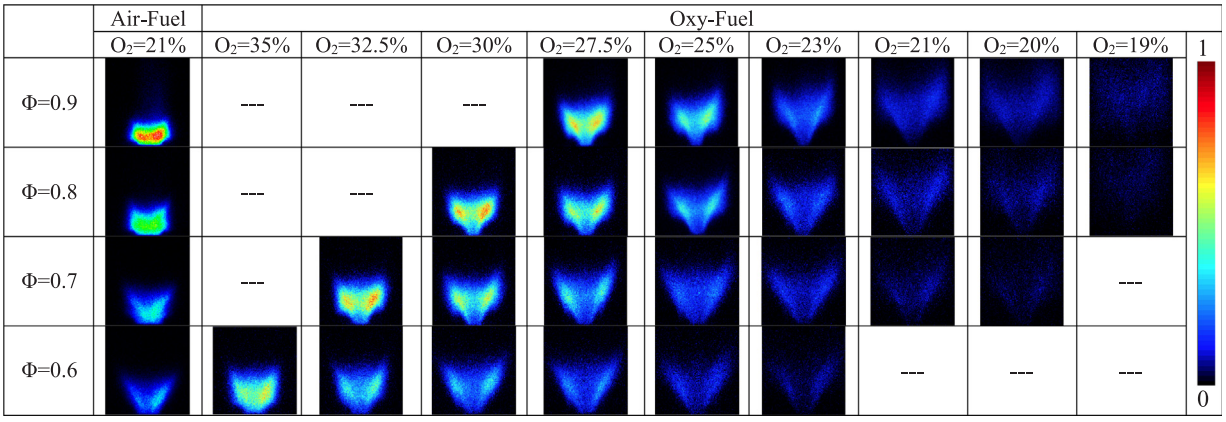

Fig. 2. OH* chemiluminescence for gaseous fuel 1 at an intensity scale of 0–1.

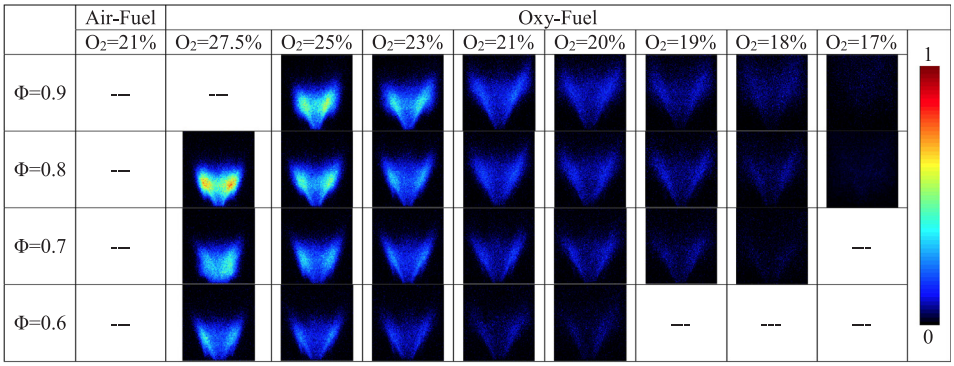

Fig. 4. OH* chemiluminescence signatures for gaseous fuel 2 at an intensity scale of 0–1.

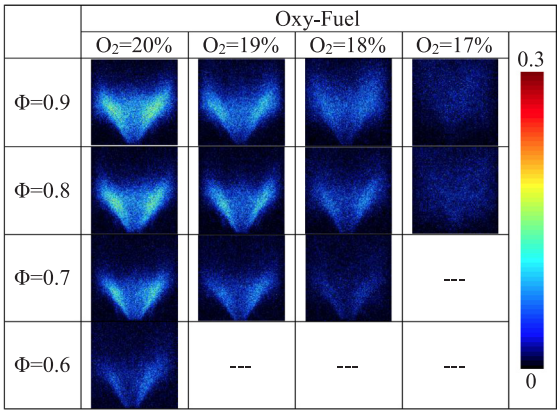

Fig. 5. OH* chemiluminescence signatures for gaseous fuel 2 at a low intensity scale of 0–0.3.

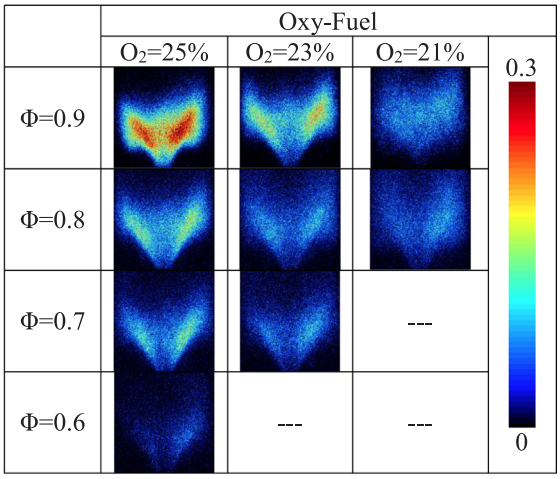

Fig. 7. OH* chemiluminescence for gaseous fuel 3 at a low intensity scale of 0–0.3.

conditions at constant heat load, heat release intensity and mixture temperature of 3.25 kW, 5.7 MW/m^3.atm and 300 K (room temperature), respectively. Equivalence ratio of the fuel-oxygen was changed from near stoichiometric (0.9) to fuel-lean mixture (0.6) condition.

4. Results and discussion

4.1. OH* chemiluminescence

Three different gaseous fuels having different volume fractions of hydrogen and methane as well as nitrogen and carbon monoxide (to obtain different low heating value gases) were utilized in the swirl-stabilized combustor. The OH* chemiluminescence signatures for each fuel were recorded, which provided the effects of fuel composition and reduced oxygen concentration on flame transition to CDC condition.

Table 3
NO emission (ppm) corrected to 15% O_2 concentration under normal air combustion.

	Φ = 0.9	Φ = 0.8	Φ = 0.7	Φ = 0.6
Gaseous Fuel 1	8.7	3.5	1.8	1.2
Gaseous Fuel 2	8.9	7.4	7.1	6.9
Gaseous Fuel 3	12	4.5	2.6	1.5

Fig. 2 shows the effect of reduced oxygen concentration in the oxidizer for gaseous fuel 1. The OH* chemiluminescence signatures obtained with normal air (21% O_2) for gaseous fuel 1 are given in the first column in Fig. 2. The flame structure changed considerably with

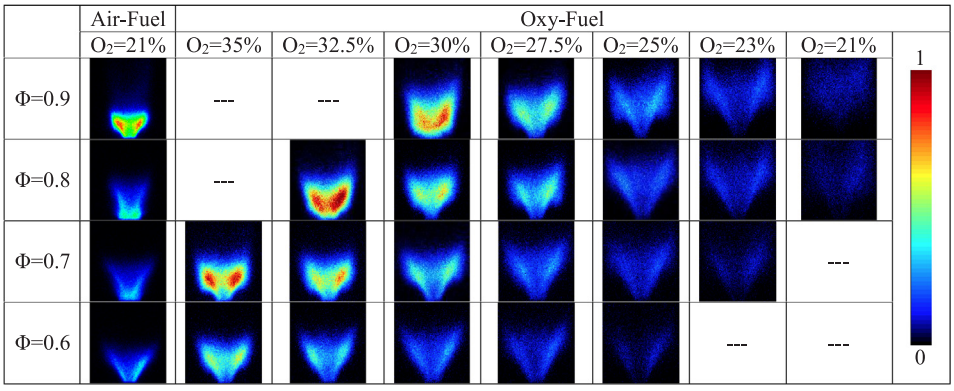

Fig. 6. OH* chemiluminescence signatures for gaseous fuel 3 at an intensity scale 0–1.

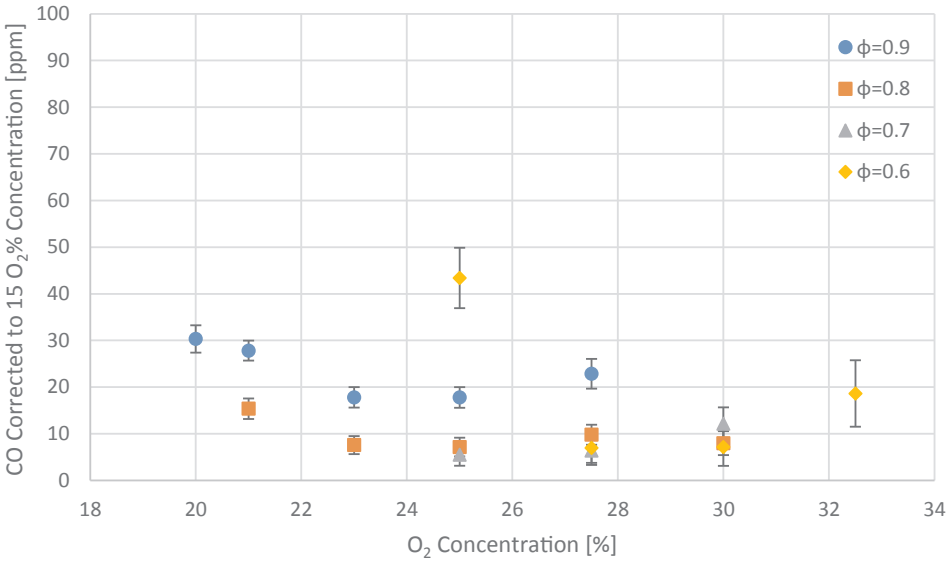

Fig. 8. CO emission (ppm) corrected to 15% O2 concentration for gaseous fuel 1.

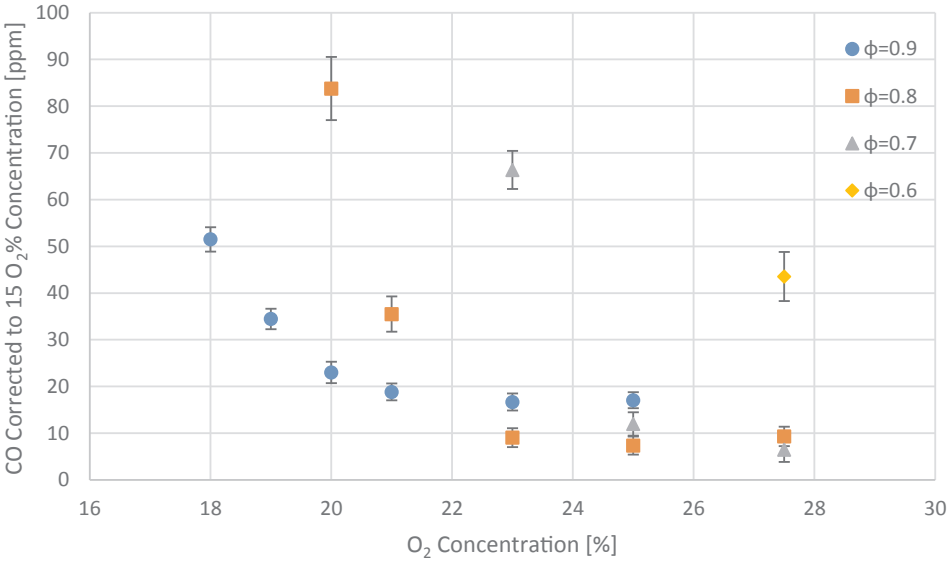

Fig. 9. CO emission (ppm) for gaseous fuel 2.

change in oxidizer from normal air to O_2-CO_2 mixture. Similar observation was made in a previous study with oxy-colorless methane combustion [18]. The oxygen concentration in the oxidizer was reduced to the lower flammability limit at each equivalence ratio.

At high oxygen concentrations (and equivalence ratios) the flames exhibited flame instabilities and flashback so that the OH* chemiluminescence are not reported under these higher oxygen concentration conditions. Higher oxygen concentrations increased lower flammability limits to allow examination at lower equivalence ratios. Thus a reduction in equivalence ratio enhanced flame stability at higher oxygen concentration. The flame structures obtained from each condition changed substantially with reduction in oxygen concentration in the oxidizer. A reduction in the oxygen concentration provided a more uniform OH* distribution over the entire reaction zone volume with the captured flame images showing more distributed behavior. In order to understand and determine the role of oxygen concentration at which transitions to CDC occurred, OH* flame signals were also displayed at a low intensity scale of 0–0.3 in Fig. 3. At $\Phi = 0.9$, for example, transition to CDC started to occur at around 20% O_2 concentration. At 19% O_2 concentration the flame stretched radially outwards to occupy a larger volume. At lower equivalence ratios similar behavior was observed except for $\Phi = 0.8$. At reduced equivalence ratios transition to CDC occurred much faster at higher O_2 concentrations. Further reduction in oxygen concentrations caused the flame to approach blow-off condition. Note that at lower equivalence ratios, the flame was not always present near the combustor walls due to much higher mixture velocities.

Fig. 4 shows OH* chemiluminescence signatures captured for gaseous fuel 2 (with scale of 0–1) that reveal the onset of oxy-colorless condition at reduced oxygen concentration. The flames obtained under normal air conditions exhibited flame instabilities and flashback so that the OH* chemiluminescence signatures are not reported for each equivalence ratio under these conditions. Flame instabilities and flashback occurred at higher oxygen concentrations since fuel 2 had higher hydrogen content (60%) compared to the other fuels examined. Flame behavior could be observed at oxygen concentration of 27.5% for $\Phi = 0.8$ to 0.6, but for $\Phi = 0.9$ only at oxygen concentration starting at ~ 25%. The flame shapes captured exhibited radial broadening with reduction in oxygen concentration in the oxidizer. Oxygen concentrations at which transition to CDC occurred were approximately 17% for

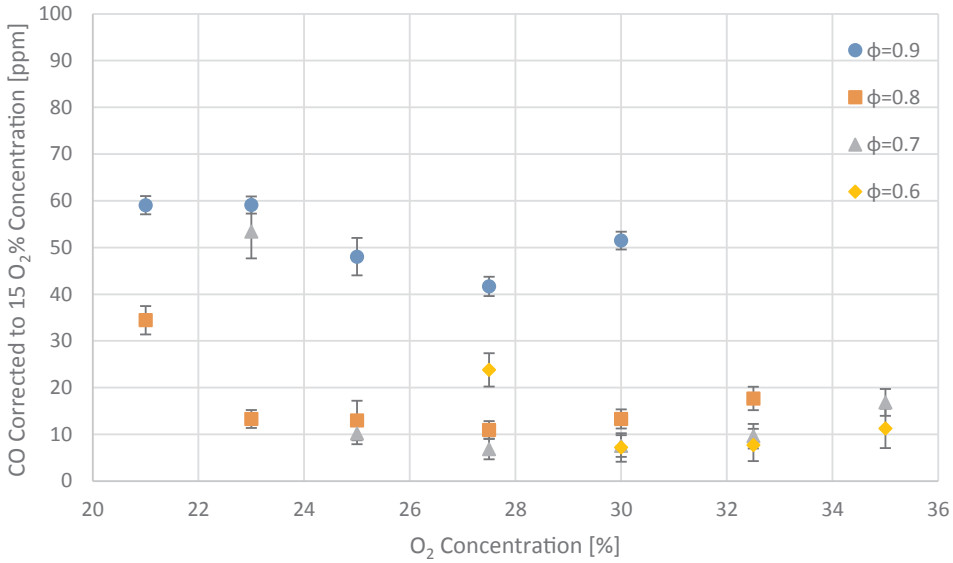

Fig. 10. CO emission (ppm) for gaseous fuel 3 ‘

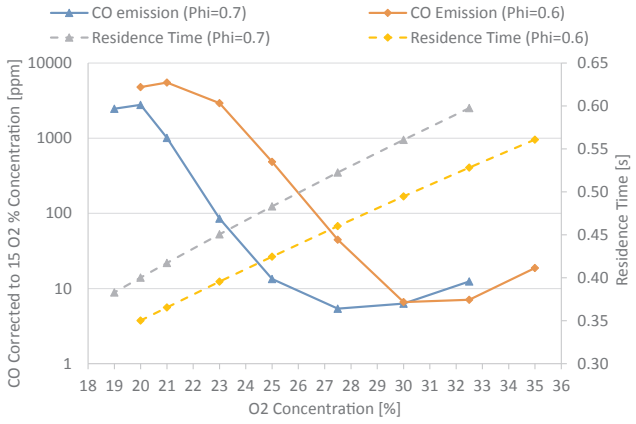

Fig. 11. CO emission vs. residence time for gaseous fuel 1.

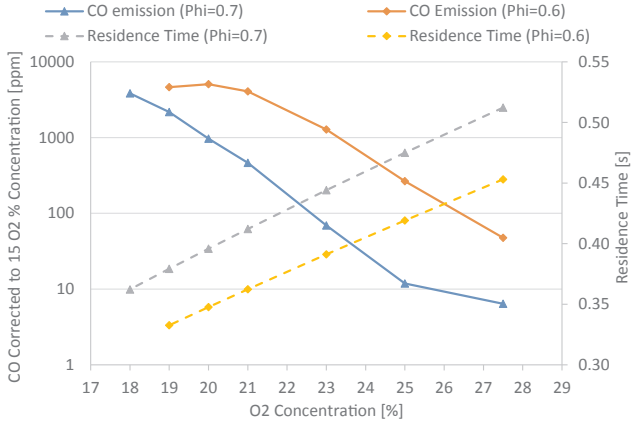

Fig. 12. CO emission vs. residence time for gaseous fuel 2.

Φ = 0.9 and Φ = 0.8 (Fig. 5). This is attributed to high hydrogen concentration in the fuel with hydrogen having much higher flame speed compared to methane. Similar results were reported in the previous study conducted by Khalil and Gupta [20]. For Φ = 0.7 and 0.6, similar flame shapes were observed for gaseous fuel 2, as with gaseous fuel 1, due to higher mixture velocities.

Fig. 6 shows OH* chemiluminescence flame signatures for gaseous

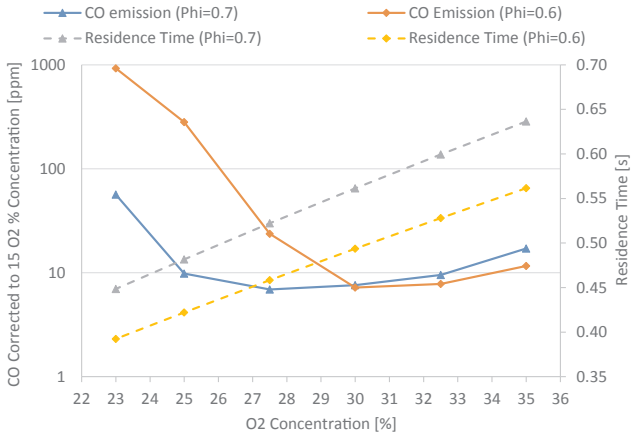

Fig. 13. CO emission vs. residence time for gaseous fuel 3.

fuel 3 which show significantly different behavior than gaseous fuels 1 and 2. The stable oxygen concentrations for each equivalence ratio were higher than of gaseous fuel 1 and 2. These findings offer direct value for fuel flexibility. Gaseous fuel 3 had greater methane concentration (40%) compared to the other fuels, which provided less flame instabilities due to flashback at higher oxygen concentration; however, at lower oxygen concentrations, flame instabilities were observed near lean blow off limits. Reduction in oxygen concentration had a strong effect on captured flame structures. Close examination of Fig. 7 reveals oxygen concentration at which transition to CDC occurred was around 21% at Φ = 0.9 and Φ = 0.8. This observation is similar to that reported in a previous study by Khalil and Gupta [18] that reported more uniform combustion at oxygen concentrations of approximately 25% and 23% using methane (100%) as the fuel, but at lower heat release intensity than reported here.

4.2. CO emission

NO_X emission was not reported, except for conventional air condition case shown in Table 3, as there was no nitrogen in the oxidizer with the oxy-fuel mixtures (i.e., using O_2-CO_2 oxidizer and fuel mixtures). Focus here was to understand the effect of reduced oxygen concentration on the CO emission along with the role of characteristic residence time. The CO emission levels were corrected to 15% oxygen

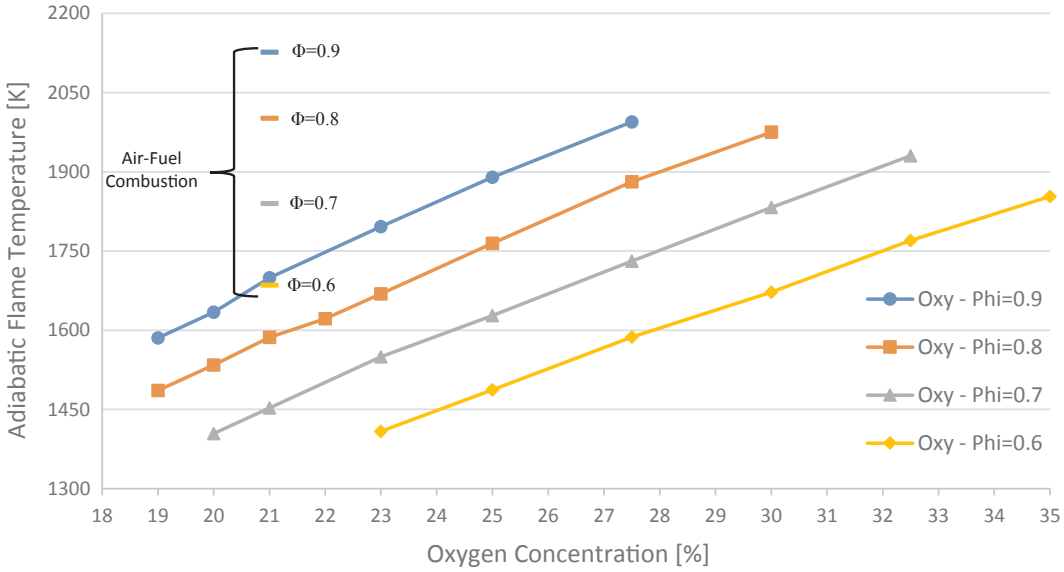

Fig. 14. Adiabatic flame temperature for gaseous fuel 1.

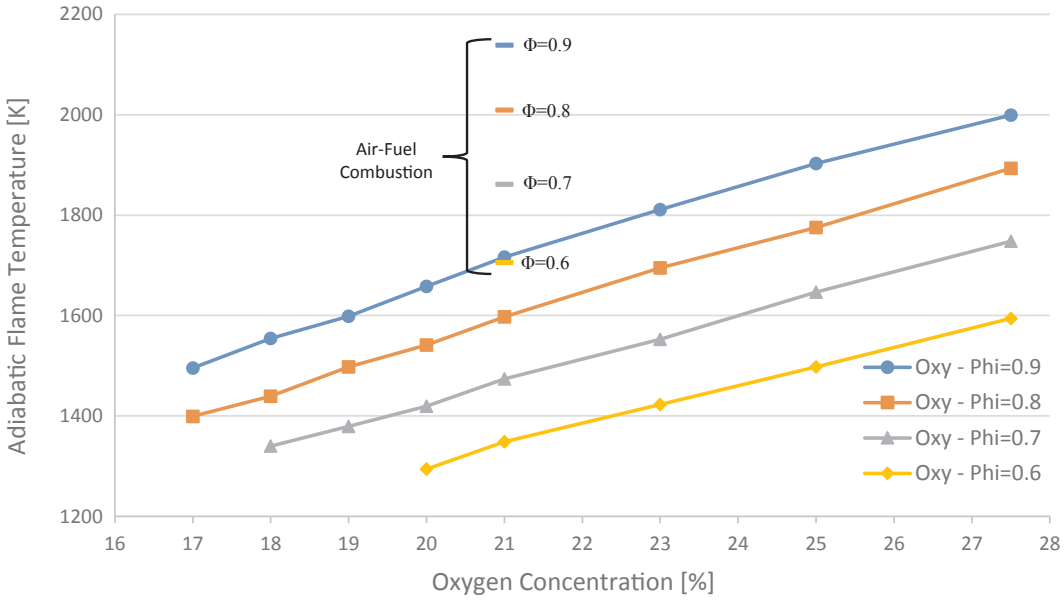

Fig. 15. Adiabatic flame temperature for gaseous fuel 2.

concentration. Correlations between CO emission measured and characteristic residence times were evaluated.

Fig. 8 shows the effect of reduced oxygen concentrations on CO emission for fuel 1 at different equivalence ratios. CO emission levels changed little at $\Phi = 0.9$, $\Phi = 0.8$ and $\Phi = 0.7$ with reduction in oxygen concentration. In particular, at $\Phi = 0.8$ and $\Phi = 0.7$, CO levels were around 10 ppm up until the lower flammability limits. Therefore, it can be concluded that reduction in equivalence ratio provides negligible effect on CO emission at these equivalence ratios. However, one can note that both reduction in the oxygen concentration and equivalence ratio led to more CO levels due to increased mixture velocity. Dissociation of CO_2 to CO also contributed to CO emission from using O_2-CO_2 as the oxidizer.

The effect of reduced oxygen concentration on CO emission for gaseous fuel 2 is given in Fig. 9. These results contrast with fuel 1, revealing CO emissions to be generally higher than fuel 1 except at higher oxygen concentrations and equivalence ratios. At $\Phi = 0.9$ and $\Phi = 0.8$, CO levels were in the range of 20–30 ppm at higher oxygen concentrations. However, CO emission increased slightly with reduction in oxygen concentration in the oxidizer. Note that fuel 2 had less methane content and CO emission were higher for fuel 2 than fuel 1 (Fig. 8) and fuel 3 (Fig. 10). We conjecture that the high hydrogen content in fuel 2 captured oxygen atoms in the oxidizer much faster during the reaction, especially at lower oxygen concentrations and equivalence ratios. Similar results on the presence of hydrogen at low mixture temperature have been reported [20]. Carbon monoxide levels for fuel 3 remained almost unchanged at reduced oxygen concentration for all equivalence ratios examined. Therefore, it can be concluded that similar hydrogen and methane concentrations in the fuel provides negligible change in CO emission levels at reduced oxygen concentration in the oxidizer. The effect of reducing equivalence ratio had negligible effect on CO emission levels.

In order to explore further higher CO levels at lower equivalence ratios and oxygen concentrations, the correlation between CO emission and the characteristic residence time was calculated. The characteristic residence time (τ) can be expressed as [32]:

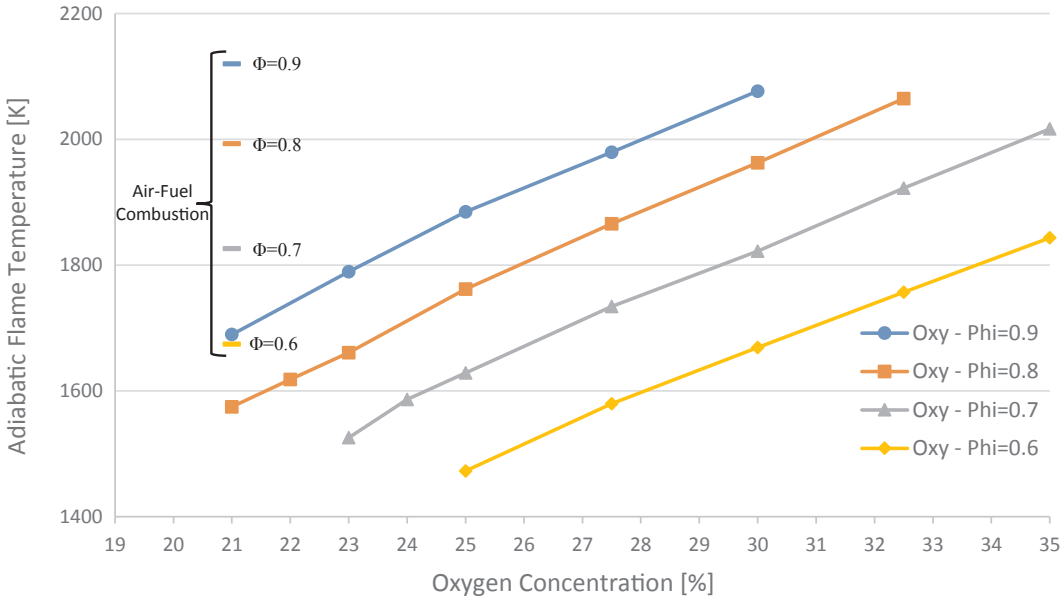

Fig. 16. Adiabatic flame temperature for gaseous fuel 3.

$$\tau = \frac{V}{\dot{Q}} \quad (1)$$

where, V is the volume of the reactor (m^3) and $\dot{Q}$ is the volumetric flow rate of the mixture (m^3/s).

The characteristic residence time for each fuel was calculated using Eq. (1) for conditions at $\Phi = 0.7$ and $\Phi = 0.6$. The correlations between the measured CO emissions and calculated characteristic residence times are presented in Figs. 11–13 for gaseous fuel 1, 2 and 3, respectively. For fuel 1, at $\Phi = 0.7$ and 0.6, the CO emission decreased slightly first, and then drastically increased with decrease in characteristic residence time. Though a similar trend was observed for fuel 2, CO emissions increased with decrease in characteristic residence time. This can be attributed to an increased presence of hydrogen in the fuel. This can also be explained from Fig. 13 which shows the correlation between measured CO levels and the characteristic calculated residence times for gaseous fuel 3. For this fuel, at $\Phi = 0.7$ and $\Phi = 0.6$, as the oxygen concentration was reduced, CO emission decreased until 30% oxygen concentration, then began to increase slightly, until near blow-off conditions wherein the CO levels increased substantially.

4.3. Adiabatic flame temperature

Adiabatic flame temperature was calculated to examine the role of reduced oxygen concentration on combustion behavior under distributed combustion condition. Chemkin-Pro [33] coupled with GRI 3.0 reaction mechanism [34] was used to determine the adiabatic flame temperatures for the normal air combustion case and oxy-fuel cases. The results are provided in Figs. 14–16 for gaseous fuels 1, 2, and 3, respectively.

Adiabatic flame temperatures at the transition points to CDC for all gaseous fuels at equivalence ratio of 0.9 having 19%, 17% and 21% O_2 concentrations, respectively) were approximately 1585 K for gaseous fuel 1, 1495 K for gaseous fuel 2 and 1689 K for gaseous fuel 3. The differences between the adiabatic flames temperatures under CDC condition from the different fuels are attributed to differences in calorific value of the gaseous fuels used. The results showed that the calculated adiabatic flame temperature decreased with reduction in oxygen concentration and equivalence ratio for all the gaseous fuels examined. The adiabatic flame temperature was approximately 20–30% lower under CDC condition as compared to normal air combustion case. This helps support the use of CDC, and also oxy-CDC, at high equivalence ratios for industrial gas turbine applications which suffers from high flame temperatures. High temperatures and hot spot zones present from combustor operation near stoichiometric equivalence ratio conditions are therefore alleviated using CDC.

5. Summary and conclusions

Oxy-colorless distributed combustion was examined here for fuel flexibility and near zero emission. Three different gaseous fuels having various hydrogen (40–60%) and methane concentrations (20–40%) along with non-reactive species (10% each of N_2 and CO_2) were utilized in a swirl-stabilized combustor under oxy-fuel distributed combustion condition. A mixture consisting of O_2-CO_2 without N_2 was used as the oxidizer for each gaseous fuel examined. Results are also reported using air as the oxidizer, which provided a baseline case. OH* chemiluminescence flame signatures for each fuel type provided the effect of reduced oxygen concentration in the oxidizer and fuel property on transition to CDC to reveal uniform distribution in the entire volume of the combustor. OH* chemiluminescence signatures showed that peak signal intensity reduced considerably for each gaseous fuel mixture with reduction in oxygen concentration in the oxidizer. At $\Phi = 0.9$, transitions to CDC initiated at oxygen concentration of 19%, 17% and 21% for gaseous fuel 1 (having 50% H_2), fuel 2 (having 60% H_2) and fuel 3 (having 40% H_2), respectively. These findings are directly attributed to the effect of hydrogen concentration in the fuel as hydrogen has higher flame speed that enhances the propensity to flashback. The presence of hydrogen in the fuel significantly affected transition to CDC without any flash back. Furthermore, oxy-colorless conditions enabled enhanced flame stability during combustion of all the gaseous fuel examined with no instability or flame flash back. At lower equivalence ratios, transition to CDC occured at higher oxygen concentrations.

The oxy-colorless conditions provided reduced CO emission; however, CO levels were somewhat higher at low equivalence ratios and oxygen concentrations due to lower mixture residence times. For gaseous fuel 1, at $\Phi = 0.8$ and $\Phi = 0.7$, CO levels remained around 10 ppm up until the lower flammability limits. CO values measured and corrected for gaseous fuel 2 were around 20 ppm at higher equivalence ratios. For gaseous fuel 3, the CO levels were 50 ppm at $\Phi = 0.9$ but reduction in equivalence ratio reduced the CO to less than 20 ppm. Lower residence time contributed to higher CO levels.

The results reveal that there are many benefits of oxy-colorless distributed combustion as a novel combustion method to achieve more uniform thermal field, very low CO emission, good fuel flexibility and no flame flash back or combustion instability. Oxy-CDC offers a beneficial approach for oxy-fuel combustion for use in industrial gas turbines, even at high (near stoichiometric) equivalence ratios. This technique also enables enhanced flame stability, in particular, for fuels having high hydrogen concentration. Oxy-colorless technique allows use of different hydrogen content gaseous fuels to provide very low CO emission and enhanced flame stability.

Acknowledgments

Office of National Research (ONR) – United States supported this research and is gratefully acknowledged by the authors. Dr. Serhat Karyeyen gratefully acknowledges the TUBITAK (The Scientific and Technological Research Council of Turkey) and Gazi University for their financial support to him as a post-doctoral research associate at the Combustion Laboratory, University of Maryland, College Park.

References

[1] Zheng L. Oxy-fuel combustion for power generation and carbon dioxide (CO_2) capture. 1st ed. Cambridge: Woodhead Publishing; 2011.
[2] Buhre BJP, Elliot LK, Sheng CD, Gupta RP, Wall TF. Oxy-fuel combustion technology for coal-fired power generation. Progr Energy Combust Sci 2005;31:283–307. https://doi.org/10.1016/j.pecs.2005.07.001.
[3] Shi B, Hu J, Ishizuka S. Carbon dioxide diluted methane/oxygen combustion in a rapidly mixed tubular flame burner. Combust Flame 2015;162:420–30. https://doi.org/10.1016/j.combustflame.2014.07.022.
[4] Galmiche B, Halter F, Foucher F, Dagaut P. Effects of dilution on laminar burning velocity of premixed methane/air flames. Energy Fuels 2011;25:948–54. https://doi.org/10.1021/ef101482d.
[5] Nemitallah M, Habib M. Experimental and numerical investigations of an atmospheric diffusion oxy-combustion flame in a gas turbine model combustor. Appl Energy 2013;111:401–15. https://doi.org/10.1016/j.apenergy.2013.05.027.
[6] Heil P, Toporov D, Forster M, Kneer R. Experimental investigation on the effect of O_2 and CO_2 on burning rates during oxyfuel combustion of methane. Proc Combust Inst 2011;33:3407–13. https://doi.org/10.1016/j.proci.2010.05.047.
[7] Ilbas M, Bektas A, Karyeyen S. Effect of oxy-fuel combustion on flame characteristics of low calorific value coal gases in a small burner and combustor. Fuel 2018;226:350–64. https://doi.org/10.1016/j.fuel.2018.04.023.
[8] Williams TC, Shaddix CR, Schefer RW. Effect of syngas composition and CO2-diluted oxygen on performance of a premixed swirl-stabilized combustor. Combust Sci Technol 2007;180(1):64–88. https://doi.org/10.1080/00102200701487061.
[9] Park S, Kim JA, Ryu C, Chae T, Yang W, Kim YJ, et al. Combustion and heat transfer characteristics of oxy-coal combustion in a 100 MWe front-wall-fired furnace. Fuel 2013;106:718–29. https://doi.org/10.1016/j.fuel.2012.11.001.
[10] Yuzbasi NS, Selcuk N. Air and oxy-fuel combustion characteristics of biomass/lignite blends in TGA-FTIR. Fuel Proc Technol 2011;92(5):1101–8. https://doi.org/10.1016/j.fuproc.2011.01.005.
[11] Riaza J, Khatami R, Levendis YA, Álvares L, Gil MV, Pevida C, et al. Combustion of single biomass particles in air and in oxy-fuel conditions. Biomass Bioenergy 2014;64:162–74. https://doi.org/10.1016/j.biombioe.2014.03.018.
[12] Peng W, Liu Z, Nezhad MM, Banisaeed M, Shahraki S, Beheshti M. A detailed study of oxy-fuel combustion of biomass in a circulating fluidized bed (CFB) combustor: Evaluation of catalytic performance of metal nanoparticles (Al, Ni) for combustion efficiency improvement. Energy 2016;109:1139–47. https://doi.org/10.1016/j.energy.2016.04.130.
[13] Bhuiyan AA, Naser J. CFD modelling of co-firing of biomass with coal under oxy-fuel combustion in a large scale power plant. Fuel 2015;159:150–68. https://doi.org/10.1016/j.fuel.2015.06.058.
[14] Smart JP, Patel R, Riley GS. Oxy-fuel combustion of coal and biomass, the effect on radiative and convective heat transfer and burnout. Combust Flame 2010;157(12):2230–40. https://doi.org/10.1016/j.combustflame.2010.07.013.
[15] Ahn S, Choi G, Kim D. The effect of wood biomass blending with pulverized coal on combustion characteristics under oxy-fuel condition. Biomass Bioenergy 2014;71:144–54. https://doi.org/10.1016/j.biombioe.2014.10.014.
[16] Li P, Dally BB, Mi J, Wang F. MILD oxy-combustion of gaseous fuels in a laboratory-scale furnace. Combust Flame 2013;160(5):933–46. https://doi.org/10.1016/j.combustflame.2013.01.024.
[17] Krishnamurthy N, Paul PJ, Blasiak W. Studies on low-intensity oxy-fuel burner. Proc Combust Inst 2009;32(2):3139–46. https://doi.org/10.1016/j.proci.2008.08.011.
[18] Khalil AEE, Gupta AK. The role of CO2 on oxy-colorless distributed combustion. Appl Energy 2017;188:466–74. https://doi.org/10.1016/j.apenergy.2016.12.048.
[19] Khalil AEE, Gupta AK. Impact of internal entrainment on high intensity distributed combustion. Appl Energy 2015;156:241–50. https://doi.org/10.1016/j.apenergy.2015.07.044.
[20] Khalil AEE, Gupta AK. Fuel property effects on distributed combustion. Fuel 2016;171:116–24. https://doi.org/10.1016/j.fuel.2015.12.068.
[21] Khalil AEE, Gupta AK. Distributed swirl combustion for gas turbine application. Appl Energy 2011;88(12):4898–907. https://doi.org/10.1016/j.apenergy.2011.06.051.
[22] Khalil AEE, Arghode VK, Gupta AK, Lee SC. Low calorific value fuelled distributed combustion with swirl for gas turbine applications. Appl Energy 2012;98:69–78. https://doi.org/10.1016/j.apenergy.2012.02.074.
[23] Khalil AEE, Gupta AK. Fostering distributed combustion in a swirl burner using prevaporized liquid fuels. Appl Energy 2018;211:513–22. https://doi.org/10.1016/j.apenergy.2017.11.068.
[24] Feser JS, Bassioni G, Gupta AK. Effect of naphthalene addition to ethanol in distributed combustion. Appl Energy 2018;216:1–7. https://doi.org/10.1016/j.apenergy.2018.02.090.
[25] Khalil AEE, Gupta AK. Thermal field investigation under distributed combustion conditions. Appl Energy 2015;160:477–88. https://doi.org/10.1016/j.apenergy.2015.09.058.
[26] Khalil AEE, Gupta AK. Internal entrainment effects on high intensity distributed combustion using non-intrusive diagnostics. Appl Energy 2015;160:467–76. https://doi.org/10.1016/j.apenergy.2015.09.053.
[27] Khalil AEE, Gupta AK. Acoustic and heat release signatures for swirl assisted distributed combustion. Appl Energy 2017;193:125–38. https://doi.org/10.1016/j.apenergy.2017.02.030.
[28] Khalil AEE, Gupta AK. Velocity and turbulence effects on high intensity distributed combustion. Appl Energy 2014;125:1–9. https://doi.org/10.1016/j.apenergy.2013.11.078.
[29] Khalil AEE, Gupta AK. On the flame–flow interaction under distributed combustion conditions. Fuel 2016;182:17–26. https://doi.org/10.1016/j.fuel.2016.05.071.
[30] Khalil AEE, Gupta AK. Towards colorless distributed combustion regime. Fuel 2017;195:113–22. https://doi.org/10.1016/j.fuel.2016.12.093.
[31] Khalil AEE, Brookes JM, Gupta AK. Impact of confinement on flowfield of swirl flow burners. Fuel 2016;184:1–9. https://doi.org/10.1016/j.fuel.2016.06.098.
[32] Sorrentino G, Sabia P, de Joannon M, Bozza P, Ragucci R. Influence of preheating and thermal power on cyclonic burner characteristics under mild combustion. Fuel 2018;233:207–14. https://doi.org/10.1016/j.fuel.2018.06.049.
[33] ANSYS CHEMKIN-PRO 19.2. ANSYS Reaction Design: San Diego; 2018.
[34] Smith GP, Golden DM, Frenklach M, Moriarty NW, Eiteneer B, Goldenburg M, et al. GRI 3.0 Mechanism. http://www.me.berkeley.edu/gri_mech/.